Energy Conversion and Management 238 (2021) 114150

Contents lists available at ScienceDirect

Energy Conversion and Management

journal homepage: www.elsevier.com/locate/enconman

Economic comparison between sCO_2 power cycle and water-steam Rankine cycle for coal-fired power generation system

Jinliang Xu [a,b], Xue Wang [b], Enhui Sun [a,b,*], Mingjia Li [c]

[a] Key Laboratory of Power Station Energy Transfer Conversion and System, North China Electric Power University, Ministry of Education, Beijing 102206, China
[b] Beijing Key Laboratory of Multiphase Flow and Heat Transfer for Low Grade Energy Utilization, North China Electric Power University, Beijing 102206, China
[c] Key Laboratory of Thermo-Fluid Science and Engineering of Ministry of Education, School of Energy & Power Engineering, Xi'an Jiaotong University, Xi'an, Shaanxi 710049, China

ARTICLE INFO

Keywords:
Supercritical carbon dioxide
Coal-fired power generation system
Boiler
Recuperator
Economic analysis

ABSTRACT

The supercritical carbon dioxide (sCO_2) coal-fired power generation system has received great attention, but its economic characteristic is not well understood. Here, we present an economic comparison when using the sCO_2 power cycle and the water-steam Rankine cycle. The triple-compression sCO_2 cycle is adopted, incorporating overlap energy utilization over entire flue gas temperature range, intercooling and double reheating techniques. The heat-resistant steel materials of boiler are carefully selected to ensure its safe operation. The cost models of sCO_2 boiler and recuperator are paid more attention. We show that the sCO_2 power system attains the net power generation efficiency of 49.01%, which is higher than 48.12% for the advanced water-steam Rankine cycle system. Compared with water-steam system, the cost of sCO_2 turbine decreases by 30.0%, but the cost of sCO_2 recuperator seems to be one magnitude larger than that of USC heater, the cost of sCO_2 boiler increase by 36.3%. Hence, the whole sCO_2 power system increases the specific cost by 29.0%. Over an entire 30 years lifetime of the power plant, the levelized cost of electricity (*LCOE*) is 60.56 $/MWh for sCO_2 power system, which decreases by 1.32% compared to water-steam system. Therefore, we declare that even though the fabrication cost increases, the sCO_2 power system is preferable to the water-steam system. The specific cost of the sCO_2 power system can be further decreased by optimization of the recuperator, which is a key component in the system.

1. Introduction

The electricity industry is the largest source of carbon emissions. The world's electrical generation from coal-fired share accounted for 36.4% of the total electrical generation in 2019. Coal-fired power will still one of the main sources of electrical generation in the foreseeable future [1]. The demand for clean and efficient coal-fired power generation technology to reduce CO_2 emission, making sCO_2 coal-fired power generation system has attracted widespread attention [2,18]. Compared with the conventional water-steam Rankine cycle, sCO_2 power cycle has obvious advantages in terms of efficiency [3], compactness [4], and corrosion resistance [5]. Therefore, the sCO_2 power cycle can be an excellent alternative to steam Rankine cycle for the future power generation. Regarding current researches, most of them focus on the different cycle layouts thermodynamic performance of the sCO_2 coal-fired power generation system [6–9]. The economy of the overall system has not been fully studied, which needs to be verified.

In the economic evaluation field of sCO_2 coal-fired power generation systems, Moullec [10] first mapped out the design of a sCO_2 coal-fired power plant with a carbon capture system, and conducted a sensitivity analysis of main component. It found that the cost of the boiler is the most important factor governing the total cost. Mecheri et al. [11] combine the power generation system optimization and economic evaluation, indicating that the single thermodynamic performance analysis is not sufficient to get the best economic solution. Park et al. [12] evaluated the power generation efficiency and levelized cost of electricity of several sCO_2 power cycle systems proposed by EDF, KIER and IAE, and the heat exchanger cost estimation adopts the calculation method proposed by KIER. Li et al. [13] did a full life cycle assessment of a 1000 MW-class sCO_2 coal-fired power plant, showing that sCO_2 coal-fired power generation system is more environmentally friendly when discussing both energy consumption and environmental pollution. Zhu et al. [14] used the weighted mass method to evaluate the cost of sCO_2 coal-fired boiler, which can reflect the boiler cost characteristics to a certain extent, and analyzed the economics of sCO_2 coal-fired units using

* Corresponding author.
E-mail address: ehsun@ncepu.edu.cn (E. Sun).

https://doi.org/10.1016/j.enconman.2021.114150
Received 6 January 2021; Accepted 6 April 2021
Available online 21 April 2021

Nomenclature

b_g	coal consumption for power supply, g·(kWh)$^{-1}$
B	coal mass, t
c_p	specific heat capacity, J·(kg·K)$^{-1}$
C	compressor
C	cost, $
CW	cooling wall
d	diameter, m
D	heating surface weight, t
E	electricity generated, kWh
EAP	external air preheater
FCI	fixed investment cost, $
g	acceleration of gravity, m·s^{-2}
G	mass flow rate, kg·(m^2·s)$^{-1}$
h	enthalpy per unit mass, kJ·kg^{-1}
H	tube height, m
HTR	high temperature regenerative heat exchanger
l_p	perimeter length of furnace, m
LTR	low temperature regenerative heat exchanger
$LCOE$	levelized cost of electricity, $·(MWh)$^{-1}$
m	mass flow, kg·s^{-1}
MTR	moderate temperature regenerative heat exchanger
N	number of devices
P	pressure, MPa
Q	thermal load, W
q	thermalload of furnace, W·m^{-2}; heat absorption per unit mass flow rate, kJ·kg^{-1}
RC	recompression cycle
s	distance between center of two neighboring tubes, m
S	area, m^2
sCO_2	supercritical carbon dioxide
SC	specific cost, $·(kW)$^{-1}$
SC	simple Brayton cycle
T	temperature, °C
T	turbine
TC	tri-compressions cycle
TCO	triple-compressions sCO_2 coal-fired power generation system based on overlap energy utilization
USC	ultra-supercritical water-steam coal-fired power generation system
w	output/ input work per unit mass, kJ·kg^{-1}
W	work, MW
x	split ratio from the total mass flow rate
ρ	density, kg·m^{-3}
λ	thermal conductivity, W· (m·K)$^{-1}$

Subscript

f	working fluid
i	inner or number 1, 2, 3…
o	outer

the levelized cost of electricity.

In the above-mentioned available studies, researchers explored the economics of sCO_2 coal-fired power generation system from various aspects. However, these studies still lack consideration of some key issues faced by the sCO_2 coal-fired power generation system. For example, the effect of large mass flow in boiler and high inlet temperature of furnace on sCO_2 boiler design and cost estimate, the influence of tremendous recuperative heat and smaller heat transfer temperature difference on the recuperator cost, and the effect of cycle layout on thermal efficiency etc. Apparently, these prerequisites will have a tremendous impact on system economic evaluation. Furthermore, compared with the latest turbine and recuperator cost models given by DOE [15], the old version overestimated the turbine cost, and the estimate of the recuperator cost was significantly lower, which is not meet the present sCO_2 coal-fired power generation system economic evaluation. Owing to these problems, the previously completed evaluations are unable to reflect the actual economy of sCO_2 coal-fired power generation system.

The present paper fills the knowledge gap in the comprehensive assessment of the economics of the sCO_2 coal-fired power generation system, and evaluates the power generation system from part to whole. The improved economic evaluation will consider the key issues faced by the sCO_2 coal-fired power generation system. In this study, the triple-compressions sCO_2 coal-fired power generation system based on overlap energy utilization (TCO) is discussed to resolve the large mass flow rate in boiler and the residual flue gas heat extraction [16,17,19], and a detailed cost model of sCO_2 boiler is constructed. The economic feasibility of TCO is quantitatively evaluated and compared with USC. Finally, through the sensitivity analysis of key economic factors, the unit economy is evaluated qualitatively. According to these analyses, the direction of improving the economy of sCO_2 cycle is pointed out.

2. Description of research cycle

2.1. sCO_2 coal-fired power generation system

For the application of sCO_2 coal-fired power generation system, facing two main problems. First, the mass flow of sCO_2 power cycle is 6 ~ 8 times larger than that of steam-water Rankine cycle, which results in non-acceptable pressure drop of boiler. Second, the sCO_2 power cycle is more suitable for medium and high temperature heat source. The flue gas temperature of boiler spans a wide temperature range from 1600 °C to 120 °C, so it is hard to achieve entire temperature range heat absorption of flue gas by a single sCO_2 power cycle. The present paper takes the TCO as the research object of sCO_2 power cycle. The following efficiency improvement strategies are adopted in TCO.

The system uses a three-stage compression to improve the cycle heat recovery effect [17]. By analogized with multi-stages steam extraction of water-steam Rankine cycle, a multi-compressions of sCO_2 power cycle is proposed to achieve the efficiency limit for cycle. Based on synergetics, RC is decoupled into two SCs. At optimal split ratio of flow rate, the two subsystems are cooperative to have no mixing induced exergy destruction and acceptable heat transfer induced exergy destruction, yielding the improved performance of RC than a single SC. Further, the TC is constructed by cooperation between RC and SC. At the main vapor parameters 620 °C/30 MPa, TC has the efficiency 52.54%, which is larger than 51.55% for RC, showing apparent efficiency amplifying. It should be emphasized that the compression stages is not infinite, the maximum stage of compressions is determined by the main vapor parameters.

The intercooling and reheating arrangement makes the cycle closer to Ericsson Cycle, which can reduce the power consumption of compressor or increase turbine output. When the turbine inlet pressure is high, the intercooling arrangement has obvious advantages. Meanwhile, the double-reheating arrangement has widely used in water-steam coal-fired power plant. Thus, the intercooling and double reheating are adopted in sCO_2 cycle.

The overlap energy utilization principle is adopted to efficiently absorb the residual heat from the tail flue. To solve the problem of boiler

flue gas heat absorption in entire temperature range, a connected-top–bottom-cycle is proposed based on cascade energy utilization and parameter coordination principles. The flue gas heat in high, moderate and low temperature scope are extracted by top cycle, bottom cycle and air preheater, respectively. Furthermore, in order to solve the drawback of efficiency gap between the top cycle and the bottom cycle when use the cascade energy utilization, the overlap energy utilization is yielded. By setting an overlap heat absorption region in high temperature flue gas, the bottom cycle can absorb part of the heat in this zone. On the premise of unchanged the efficiency of the top cycle, the efficiency gap between the top cycle and the bottom cycle is filled, the whole system efficiency is improved [16].

The partial flow applied to sCO_2 boiler to decrease the flow resistance [19]. The boiler partial flow means that separate the total mass flow of working fluid into two parts having identical mass flow for each, and then they flow through different heating surfaces of the boiler. Under the condition that the total mass flow and enthalpy increase unchanged, the partial flow mode reduces the pressure drop to 1/8 of the total flow mode. The results show that sCO_2 boiler pressure drop can be equivalent to or even smaller than that for USC boiler. For tube wall temperature control of boiler, the heat load matching strategies used for sCO_2 boiler to reduce tube temperature of the boiler. It means working fluid enters from the place where the heat load is higher in the furnace.

Through the combination of the above innovations, constructed cycle efficiency represents the maximum level of sCO_2 coal-fired power generation system, which can be used for comparative study with advanced USC. With vapor parameters 600 °C/620 °C/620 °C/31 MPa, TCO power generation efficiency can reach 49.01%, showing superiorities over water-steam Rankine cycle [20–21].

The system layout is shown in Fig. 1. The working process of the cycle is that the supercritical carbon dioxide is split at the outlet of the low-pressure side of MTR, part of the working fluid enters the low-pressure side of LTR, and the other part enters compressor 4 (C4). The working fluid entering the LTR is further diverted at the low-pressure side outlet of the LTR, and partially into the cooler 1, C1, cooler 2, and C2 in turn, and then enters the high-pressure side of the LTR, and the other portion enters the C3, after being compressed by C3, it merges with the working fluid at the high-pressure side outlet of the LTR and enters the MTR. At the exit of MTR, it merges with the working fluid compressed by C4 and then diverges. One part enters HTR and the other part enters HTR2. The working fluid entering HTR enters heater1 to absorb heat, and the other part enters heater4a and heater4b through the high-pressure side of HTR2. And then merges with the working fluid at the exit of heater1, the combined working fluid enters T1, heater2, T2, heater3, and T3 in turn, and then splits again at T3 outlet. One of them enters the low-pressure side of HTR, and the other enters the low-pressure side of EAP and HTR2. The two working fluids enter the MTR after converging at the outlet of the low-pressure side exit of HTR, then, the working fluid completes a cycle.

2.2. Advanced ultra-supercritical water-steam coal-fired power generation system

The 1000 MW double-reheating USC unit in the Laiwu Power Plant evaluated at present work is shown in Fig. 2. A new 10 feedwater heater configuration (four HP heater, one deaerator, five LP heater, and one two-stage steam condenser) are adopted in the unit to improve efficiency. After the 10 heaters, the economizer inlet feedwater temperature is 319 °C. For conventional USC boilers, the heating surface pattern is total flow mode. All working fluid enters the furnace, and then passes through the economizer, water wall, superheater and reheater to absorb heat. The steam parameters of Huaneng Laiwu Power Plant are 600 °C/620 °C/620 °C/31 MPa, and the power generation efficiency reaches 48.12% [20], representing the highest efficiency of the double-reheating USC unit currently in operation.

3. Calculation method

3.1. Thermodynamic calculation of sCO_2 power cycle

In this study, thermodynamic analysis and modeling are performed using FORTRAN, NIST REFPROP was used for working fluid physical property database. Fig. 3 shows the computation scheme. Table 1 lists important parameters for TCO cycle computation in this paper. Shown in Fig. 1, once thermodynamic parameters at various state points are obtained, net power per unit mass flow rate of CO_2 (w_{net}), heat absorption per unit mass flow rate of CO_2 (q_{total}) are

$$w_{net} = (w_{T1} + w_{T2} + w_{T3}) - (w_{C1} + w_{C2} + w_{C3} + w_{C4}) \quad (1)$$

$$q_{totle} = (1 - x_{Heater4})(h_8 - h_7) + x_{Heater4}(h_8 - h_{6b}) + (h_{10} - h_9) + (h_{12} - h_{11}) - x_{EAP}(h_{13} - h_{13b}) \quad (2)$$

where $x_{Heater4}$ is the ratio of flow rate in Heaters 4a and 4b to the total flow rate, x_{EAP} is the ratio of flow rate in EAP to the total flow rate.

The overall system thermal efficiency (η_{th}), which is defined as the

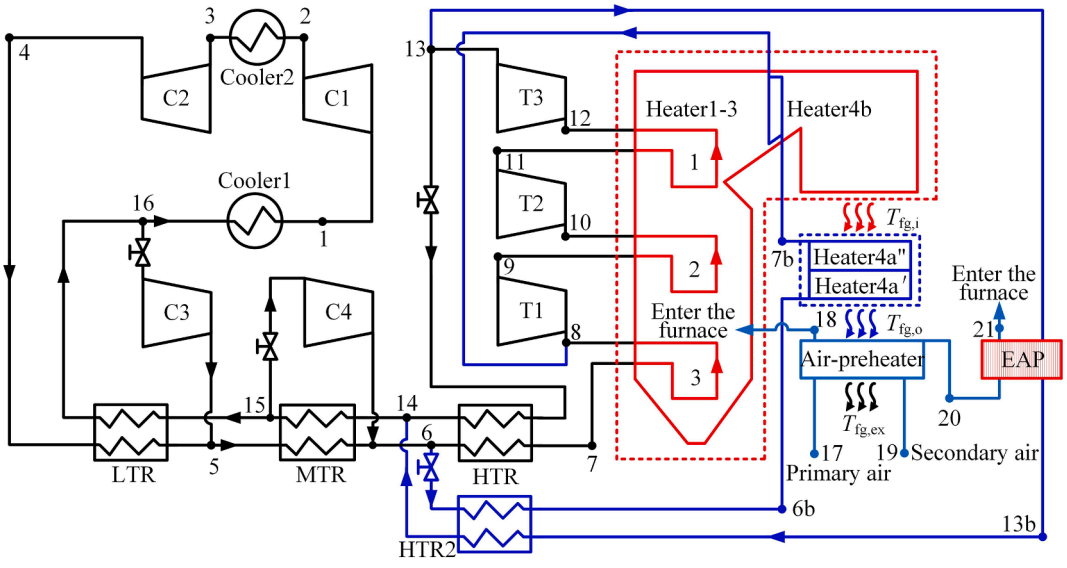

Fig. 1. Triple-compression sCO_2 coal-fired power generation system with overlap energy utilization (TCO).

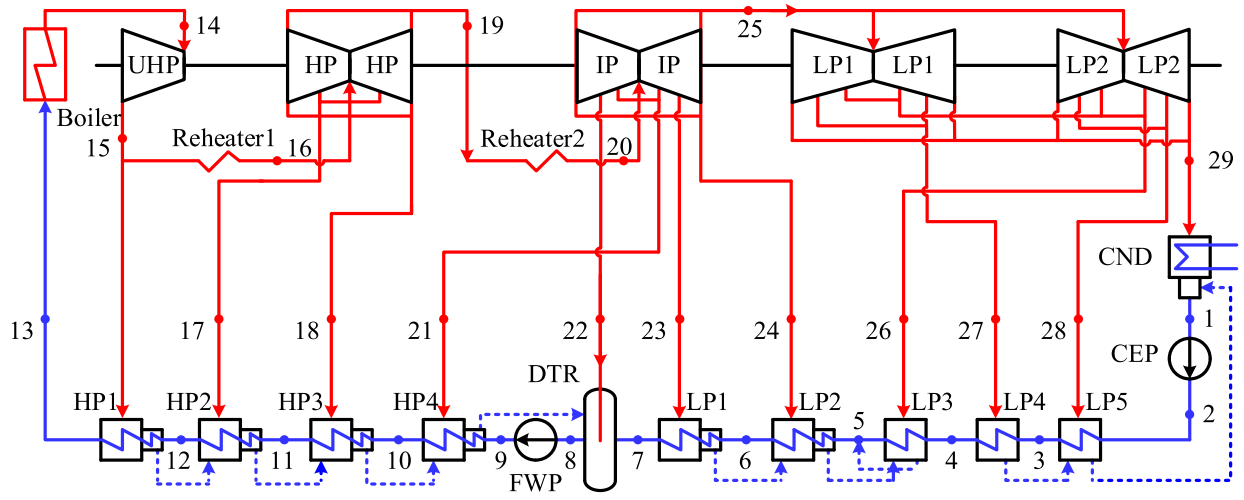

Fig. 2. State of the art ultra-supercritical water-steam coal-fired power generation system (USC) of Huaneng Laiwu.

ratio of w_{net} and q_{tota}, is adopted here to evaluate the thermodynamic performance and is represented as:

$$\eta_{th} = \frac{w_{net}}{q_{totle}} \tag{3}$$

3.2. Coupling calculation of sCO_2 boiler

Given the boundary conditions of the cycle, the boiler calculation model is obtained through the coupling of furnace thermal calculation and cooling wall aerodynamic calculation [16,17,19,22]. Based on coupling model, structural parameters and layout of the boiler cooling wall are determined, the pressure drop of the working fluid on the furnace side is calculated, and the tube wall temperature of cooling wall is checked. The influence of the unevenness of the heat load along the furnace width and furnace depth is ignored, and the one-dimensional heat transfer model along the furnace height is used.

The average heat flux of furnace is

$$q_{ave} = Q_{FUR}/S_{FUR} \tag{4}$$

where Q_{FUR} and S_{FUR} are thermal load and heat transfer area in furnace. When the thermal load non-uniform coefficient (η_i) along the height of the furnace is provided, the thermal load distribution along the height direction (q) in the furnace is:

$$q = q_{ave} \cdot \eta_i \tag{5}$$

According to the furnace thermal calculation, the thermal load distribution in the furnace can be determined, and the tube height of each part of the cooling wall can be obtained by energy conservation calculation. As the thermal load and the physical properties of the working fluid in the tube are constantly changing along the furnace height, the CW module is uniformly discrete along the furnace height into n micro-element calculations [22]:

$$\begin{cases} \sum H(i)q(i)l_p = c_p m_f (T_{out} - T_{in}) \\ H = \sum H(i) \end{cases} \tag{6}$$

where H, q, p, c_p, m, T_{out}, T_{in} are tube height, heat flux, perimeter length of furnace, working fluid specific heat capacity, mass flow in each tube, outlet and inlet temperature of CW in section i.

The thickness of the tube is calculated and determined according to China's current national standards for water boilers [23]:

$$\delta = \frac{Pd_i}{2\varphi_{min}[\sigma] - P} + c \tag{7}$$

In Eqs. (7), P is the calculated working fluid pressure; d_i is the tube inside diameter, $[\sigma]$ is the allowable stress of metal, φ_{min} is the minimum attenuation coefficient, taken as 1, c is the additional thickness.

When the working fluid flows in the tube, its pressure drop is generally composed of four parts, which are frictional pressure drop, local resistance pressure drop, gravity pressure drop and accelerated pressure drop. Since the acceleration pressure drop is relatively small and can be ignored, the total pressure drop of the tube can be written as:

$$\Delta P = \Delta P_f + \Delta P_{jb} + \Delta P_g \tag{8}$$

Equations (9) and (10) are pressure drop due to the gravity and friction, where ρ is the working fluid density, g is the acceleration of gravity, l is the length of the tube, G is the mass flow rate, the friction factor f is calculated according to Filonenko formula [24], Where Re is the Reynolds number.

$$\Delta P_g = \rho_f g H \tag{9}$$

$$\Delta P_f = \frac{1}{2} f \frac{l}{d_i} \frac{G^2}{\rho_f} \tag{10}$$

$$f = \frac{1}{(1.82 lg Re_f - 1.64)^2} \tag{11}$$

Various tube fittings such as elbows and valves are installed in the pipeline system. When fluid flows through these tube fittings, a local resistance pressure drop occurs, which is mainly determined by experiments. When calculation involves the local resistance pressure drop, the program calculation only includes the main local resistance pressure drop. Then there is

$$\Delta P = \frac{1}{2} \frac{G^2}{\rho_f} \left(\frac{l}{d_i} \frac{1}{(1.82 lg Re_f - 1.64)^2} + \xi_{jb} \right) + \rho_f g H \tag{12}$$

$$R = \frac{l}{d_i} \frac{1}{(1.82 lg Re_f - 1.64)^2} + \xi_{jb} \tag{13}$$

where ξ_{jb} is the local resistance coefficient, R is the converted resistance coefficient.

The sCO_2 temperature in the cooling wall is relatively high, and it is always far away from the pseudo-critical area. The physical properties of the working fluid change smoothly, which is similar to a constant physical properties fluid. Thus, D-B formula [25] is used to calculate the working fluid convective heat transfer coefficient α_f,

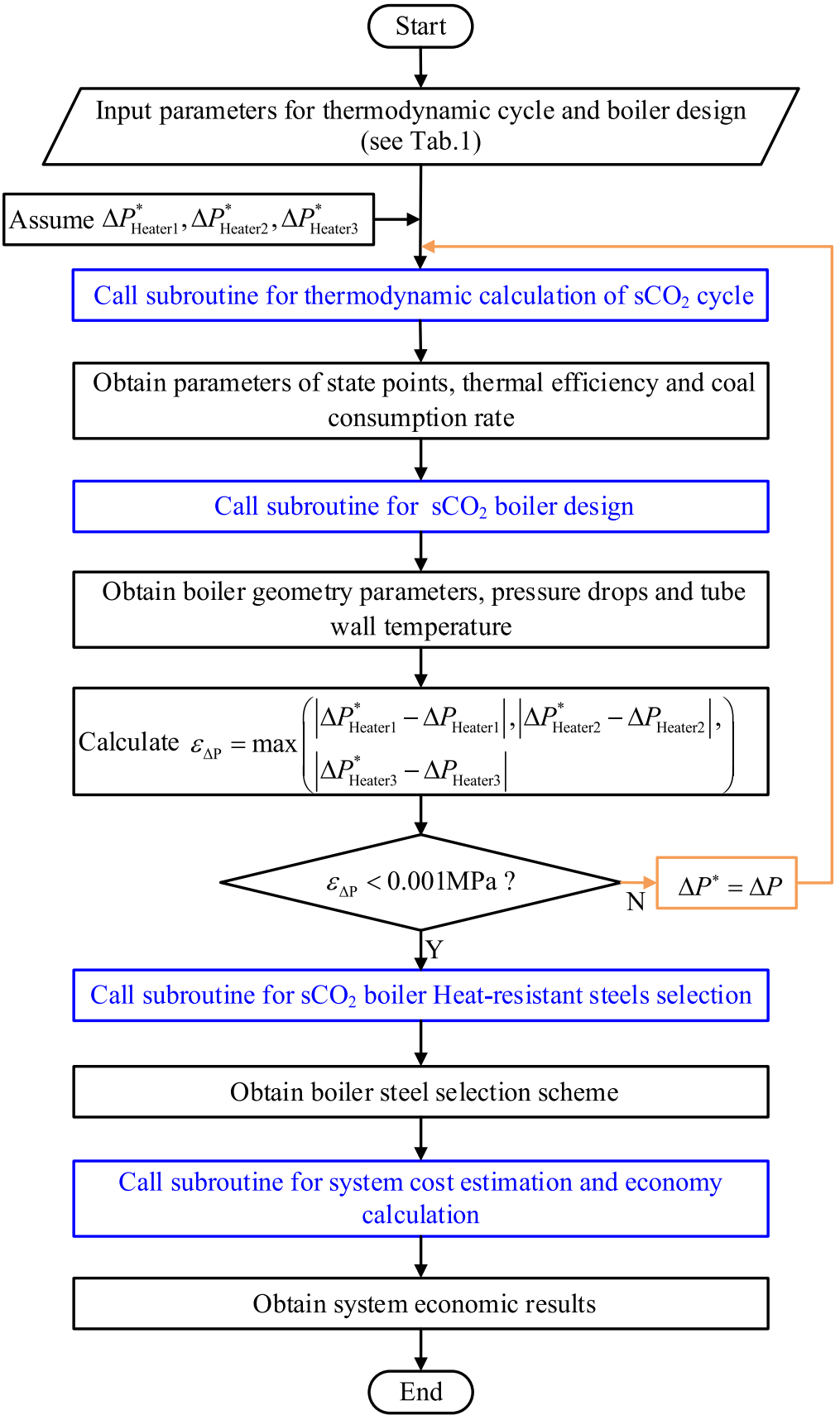

Fig. 3. Calculation process of sCO_2 economic evaluation.

Table 1
Parameters related to the calculation of the coupling between the sCO_2 cycle and the boiler.

Parameters	Values
turbine inlet temperature(T_8)	600 °C
turbine inlet pressure(P_8)	31 MPa
reheating temperature	620/620 °C
turbine isentropic efficiency ($\eta_{T,s}$)	93%
compressor C1 inlet temperature(T_1)	32 °C
compressor C1 inlet pressure(P_1)	7.6 MPa
compressors isentropic efficiency ($\eta_{C,s}$)	89%
pressure drops in LTR and HTR (ΔP)	0.1 MPa
LTR and HTR pinch temperature difference (ΔT_{LTR} or ΔT_{HTR})	10 °C
primary air temperature($T_{pri\ air}$)	320 °C
fresh air temperature entering air-preheater($T_{pri\ air,in}$)	31 °C
ratio of primary air flow rate to the total air flow rate	19%
cold secondary air temperature($T_{sec\ air,in}$)	23 °C
secondary air flow rate ratio	81%
excess air coefficient	1.2
flue gas outlet temperature ($T_{fg,\ ex}$)	123 °C
environment temperature (T_e)	20 °C

$$\alpha_f = \frac{\lambda_f}{d_i} 0.023 Re_f^{0.8} Pr_f^{0.4} \tag{14}$$

In Eqs. (14), λ is the thermal conductivity, Pr is the Prandtl number. Under the given heat load distribution, the temperature of the inner and outer walls of the cooling wall (T_i and T_o) is calculated by Fourier's law [26]. The equivalent heat flux q_{equiv} is related to the outer surface of the tube and can be determined by the following relationship. The calculated tube wall temperature T_c used for strength calculation and tube steel selection is showed in Eqs. (18) [27]

$$T_i = T_f + \frac{q_{equiv} \cdot d_o}{d_i \cdot \alpha_f} \tag{15}$$

$$T_o = T_i + \frac{q_{equiv} \cdot d_o}{2\lambda} ln\frac{d_o}{d_i} \tag{16}$$

$$q_{equiv} = \frac{q \cdot \left(s - d_o + \pi \cdot \frac{d_o}{2}\right)}{\pi d_o} \tag{17}$$

$$T_c = \frac{T_i + T_o}{2} \tag{18}$$

3.3. Model validation

Since there are no test data for the temperature field of the sCO_2 boiler cooling wall, the operating data of a supercritical water-steam boiler in a Poland power plant are used to verify the accuracy of the proposed mathematical model [29]. The detailed design parameters of the boiler are listed in Table 2. In the validation, the steady-state data in the literature are used for calculation. The heat load distribution along the height direction of the tube is consistent with the literature, and the convective heat transfer coefficient is the same as the formula in the original literature. Fig. 4 shows the mainstream temperature of the working fluid T_f and the temperature of the inner and outer walls along the length of the tube. The solid line represents the calculation results, and the solid dots represent the data in the reference. It can be seen that the calculation results in this study are qualitatively matched with the data reported in the literature, the wall temperature deviation is less than 1.86 °C, and the main stream temperature deviation is less than 2.48 °C. Therefore, the calculation model in this paper is reasonable and reliable.

3.4. Cost estimation for sCO_2 coal-fired power generation system

The cost of the boiler is determined by the weight and price of various heat-resistant steel. Where D is the heating surface weight, p is the steel price ratio (based on the price of T91 steel, see Table 3) [30,31], C_{BW} is the price of the traditional ultra-supercritical water-steam coal-fired boiler.

$$C_{Bs\text{-}co2} = C_{BW} \frac{\sum p_{S\text{-}CO2,i} \cdot D_{S\text{-}CO2,i}}{\sum p_{USC,i} \cdot D_{USC,i}} \tag{19}$$

Up to date, the structural parameters of the double-reheating USC unit boiler are hard to obtain such as tube formats, tube material, etc., which makes the absence of reference information. The calculation of the sCO_2 boiler cost is based on the available data for single-reheating USC boiler. The cost of single-reheating water boiler is closed to double-reheating. Table 5 shows the heating surface structural parameters of the single-reheating USC unit boiler in the literature [27]. The reasonable cost estimation of the sCO_2 boiler is carried out by referring

Table 2
Parameters related to the validation of the supercritical boiler.

Parameters	Values
boiler basic information	BB2400 supercritical boiler with capacity 2400 t/h of live steam with 26.6 MPa/554 °C
total mass flow rate	2270 t/h
number of waterwall tubes	768
tube length	165 m
inlet pressure of waterwall	29.9 MPa
inlet temperature of waterwall	315 °C
Waterwall tube formats ($d_o \times \delta$)	33.7 × 6.3 mm 38.0 × 6.3 mm (above 49.4 m)
tube pinch of waterwall	50 mm 57 mm (above 49.4 m)
Tube inclination angle of waterwall	$a_1 = 24.62°$ $a_2 = 28.36°$ (above 49.4 m)
tube material of waterwall	16Mo3 13CrMo45(above 49.4 m)

Note: above 49.4 m refers to the vertical upward boiler height from half of the cold ash hopper.

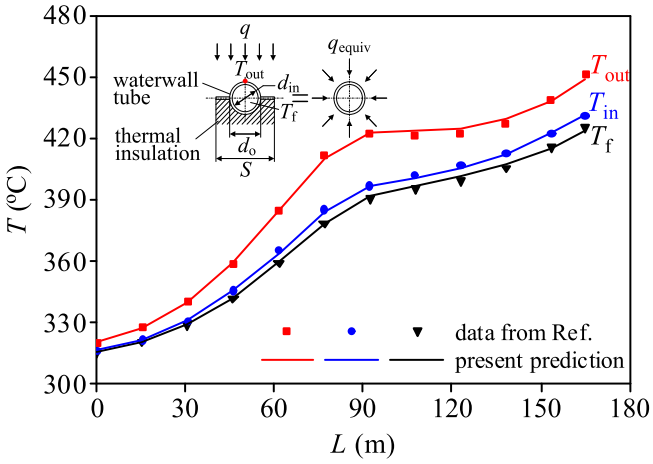

Fig. 4. Comparison of literature value and calculation model results in this paper.

Table 3
Price ratio of end products of boiler heating surface tube.

Steel	Price ratio
12Cr1MoV	0.435
SA213T23	0.87
SA213T91	1
TP347H	3.25
Super 304H	2.75

to the data of Reference Cost Index of Thermal Power Project Quota Design (Level 2017) provided by China Electric Power Planning & Engineering Institute (EPPEI) [32].

The turbine cost is given by NETL [15], where f_T is a temperature correction factor that takes into account the material selection and thickness changes with temperature.

$$C_t = 182600 W_T^{0.5561} \times f_{T,t} \tag{20}$$

$$f_T = \begin{cases} 1, T_{max} \leqslant 550C \\ 1 + 1.106 \times 10^{-4} (T_{max} - 550)^2, T_{max} \geqslant 550C \end{cases} \tag{21}$$

Compressor cost [15] is

$$C_c = 1230000 W_{sh}^{0.3992} \tag{22}$$

where W_T is the turbine work and W_{sh} is the compressor shaft work.

Recuperator and direct air cooler costs [15], are

$$C_{Recup} = 49.45 UA^{0.7544} \times f_{T,Recup} = 49.45 \left(\frac{Q_{Recup}}{\Delta T_{int}} \right)^{0.7544} \times f_{T,Recup} \tag{23}$$

$$T_{max} = \begin{cases} 1, T_{max} \leqslant 550C \\ 1 + 0.02141 (T_{max} \geqslant 550C) \end{cases} \tag{24}$$

$$C_{cooler} = 32.88 UA^{0.75} = 32.88 \left(\frac{Q_c}{\Delta T_{int}} \right)^{0.75} \tag{25}$$

where ΔT_{int} is the integral average temperature difference of heat exchanger, Q is the thermal load, UA is the ratio of the heat exchanger heat load to the integral average temperature difference. In this paper, the recuperator type of sCO_2 cycle is PCHE. Here, it should also be noted that the equipment cost of the USC unit will consult to the actual data provided by EPPEI, thus the detailed USC unit cost calculation will not be carried out in this paper.

3.5. Economic calculation of power generation system

The economic computation will further evaluate the rationality and cost-effectiveness of the system, taking into account several economic indicators, which is the specific cost (*SC*), the coal consumption for power supply (b_g) and the levelized cost of electricity (*LCOE*) of the power generation system. The economic assumption and index were made to estimate them, which are specified in Table 4.

SC is a commonly used indicator for evaluating the fabrication cost of power generation systems [33]. It represents the unit cost of per electrical kilowatt installed capacity of the power plants and provides a qualitative concept for comparing similar systems.

$$SC = \frac{C_{tot}}{W_{net}} \tag{26}$$

$$C_{tot} = \sum_{j=1}^{NHX} C_{HX,j} + \sum_{j=1}^{NT} C_{T,j} + \sum_{j=1}^{NC} C_{Com,j} + \sum_{j=1}^{NA} C_{A,j} \tag{27}$$

$$C_j = c_{inst,j} \cdot C_{equip,j} \tag{28}$$

where C_{tot} is the total investment cost of the system includes not only the cost of the main equipment of the system, but also the cost of auxiliary equipment and installation costs, W_{net} is the total installed capacity of the power plant, C_{equip}、c_{inst} are the equipment purchase costs and cost factors considering installation materials, workers, electricity, transportation, etc.

b_g is one of the main indicators for the economic evaluation of coal-fired power plants. It refers to the average standard coal consumption of per kilowatt-hour of electricity during the statistical period, which can be determined by the following formula [34]:

$$b_g = \frac{B_b \times \left(1 - \frac{\alpha}{100}\right)}{E_{gen} \times \left(1 - \frac{L_{fcy}}{100}\right)} \times 10^6 \tag{29}$$

B_b is the standard coal consumption, which is the amount of fuel used converted to standard coal in the statistical period, L_{fcy} is the auxiliary power consumption rate, E_{gen} is the electricity generated, α is the heating ratio.

The standard investment of power generation is analyzed by *LCOE*, which is estimated by using the total revenue requirement (TRR) method and thermodynamic analysis results [35], including fabrication cost and operation cost of power plant. It is defined as the sum of annual investment cost, annual operation and maintenance (O&M) cost, and annual fuel cost of the plant divided by the annual electricity production. The plant's lifespan is assumed 30-year.

$$LCOE = \frac{(CRF \times FCI + C_{OM} + C_f)}{8760 \cdot w \cdot W_{net}} \tag{30}$$

$$FCI = (1 + c) \cdot b \cdot C_{tot} \tag{31}$$

$$CRF = \frac{k \cdot (1 + k)^n}{(1 + k)^n - 1} \tag{32}$$

$$C_c = b_g \cdot W_{net} \cdot 8.76 \cdot w \cdot c_{coal} \tag{33}$$

$$C_{OM} = C_{F\text{-}OM} + C_{V\text{-}OM} \tag{34}$$

where b is the process contingency cost coefficient, which aims to compensate for the insufficient cost estimation caused by the uncertainty of the technological development status, c is the project contingency cost coefficient, which refers to the data given by NETL [36].*CRF* is the investment recovery factor related to the discounted rate k and the lifespan of equipment *NY*. O&M costs are divided into two parts: fixed cost $C_{F\text{-}OM}$ that is independent of operating time of the plant, and variable cost $C_{V\text{-}OM}$ that is proportional to power generation, such as waste treatment, maintenance materials, etc.

Table 4
Assumptions and value for economic analysis [35].

Parameters	Values
coal price(c_{coal})	119.56 $/t
lifetime of the power plant (*NY*)	30 yr
annual utilization factor of power plant (w)	0.85
discount Rate (k)	12%
inflation rate(α)	2%

4. Results and discussion

4.1. TCO and USC boiler heating surfaces layout

The heat-resistant steel system that takes into account both strength and corrosion resistance has been maturely applied to the field of ultra-supercritical water-steam coal-fired power generation and nuclear power. These materials have become the optional objects for key components of the sCO_2 coal-fired power generation system, and the corrosion and compatibility test of sCO_2 is ongoing. Refer to the commonly used steels in power plant water-steam boiler, under the premise of long-term safe and reliable operation of the plants, the material selection scheme for the sCO_2 boiler cooling wall will obtain from the perspective of the high-temperature strength and the corrosion characteristics of materials [28,30,31,37]. In this study, we will focus on meeting the demand of steel high-temperature strength, so as to avoid overheating of heating surface of sCO_2 boiler. According to the heat-resistant steel selection, the allowable stress of heat-resistant steels at the operating temperature is required to be no less than 49 MPa. Guided by the design criteria of typical coal-fired boilers, the feasibility of

Table 5
TCO and reference single-reheating USC boiler heating surfaces.

TCO					USC				
Heating surfaces	Tube formats (mm)	Materials	Tube numbers	Weights (t)	Heating surfaces	Tube formats (mm)	Materials	Tube numbers	Weights (t)
Part1	ϕ41.16 × 8.33	SA213T91	1943	165.47	Radiation zone under furnace (SWW)	ϕ 38.1 × 6.7	SA213T23	1592	258.39
Part2	ϕ41.11 × 9.06	SA213T91	1946	113.04	Radiation zone upper furnace	ϕ31.8 × 6.7	SA213T23	1592	219.66
Part3	ϕ31.82 × 5.91	SA213T91	2514	42.50	Horizontal low temperature SH (HLSH)	ϕ50.8 × 8.4	SA213T23	1200	1181.38
Part4	ϕ51.20 × 9.10	SA213T91	1589	128.92	Vertical low temperature SH (VLSH)	ϕ50.8 × 8.9	SA213T23	1200	98.64
Part5	ϕ54.18 × 9.59	SA213T91	1476	169.49	Partition screen SH (PSH)	ϕ60.3 × 9.3	TP347H	754	192.70
Part6	ϕ ϕ51.95 × 9.48	SA213T91	1406	166.48	Rear screen SH (RSH)	ϕ63.5 × 7.5	Super 304H	754	170.63
SH1	ϕ51.95 × 9.48	Super 304H	1560	277.04	High temperature SH (HSH)	ϕ57.1 × 6.8	Super 304H	1504	251.99
SH1	ϕ51.95 × 9.48	Super 304H	1560	277.04	Horizontal low temperature RH (HLRH)	ϕ63.5 × 5.7	SA213T23	1440	1096.89
RH1	ϕ51.21 × 5.60	Super 304H	3108	934.87	Vertical low temperature RH (VLRH)	ϕ63.5 × 3.6	TP347H	1440	76.05
RH2	ϕ51.21 × 5.60	Super 304H	2814	104.36	High temperature RH (HRH)	ϕ60.3 × 3.5	Super 304H	1062	206.84
RH3	ϕ55.81 × 8.40	Super 304H	2733	213.50	Economizer (ECO)	ϕ45.0 × 6.6	SA210C	–	–
RH4	ϕ55.81 × 8.40	Super 304H	1440	253.10					
Heater4b	ϕ 34.52 × 7.26	Super 304H	1083	294.40					
Heater4á	ϕ43.0 × 9.00	12Cr1MoV	2820	2157.61					
Heater4a“	ϕ41.0 × 8.00	SA213T23	2460	1623.52					

applying T23, T91, P92, Super304H, HR3C, Inconel625, etc. to sCO_2 boilers under material boundary conditions is studied. Fig. 5 shows the variation of bulk temperature with tube wall thickness under the identical heat load and material boundary conditions. The results demonstrate that when the sCO_2 cycle is adopted, mainly because of the high temperature of the working fluid at the entrance of the furnace, the steel grade of the CW needs to be improved, and the ferrite such as 12Cr1MoVG, T21 and T23 cannot be used in the CW. For the double-reheating sCO_2 cycle, the temperature of the working fluid at the furnace inlet is above 510 °C, while the double-reheating steam Rankine cycle is only about 320 °C[20]. Under the same wall thickness, it can be seen from wall temperature formula that the temperature of the inner and outer walls of the sCO_2 cycle will be higher. Moreover, to ensure acceptable boiler pressure drop, the sCO_2 boiler cooling wall should choose a slightly larger tube inside diameter, which yield an increment of tube thickness and further increase the wall temperature. Thus, the

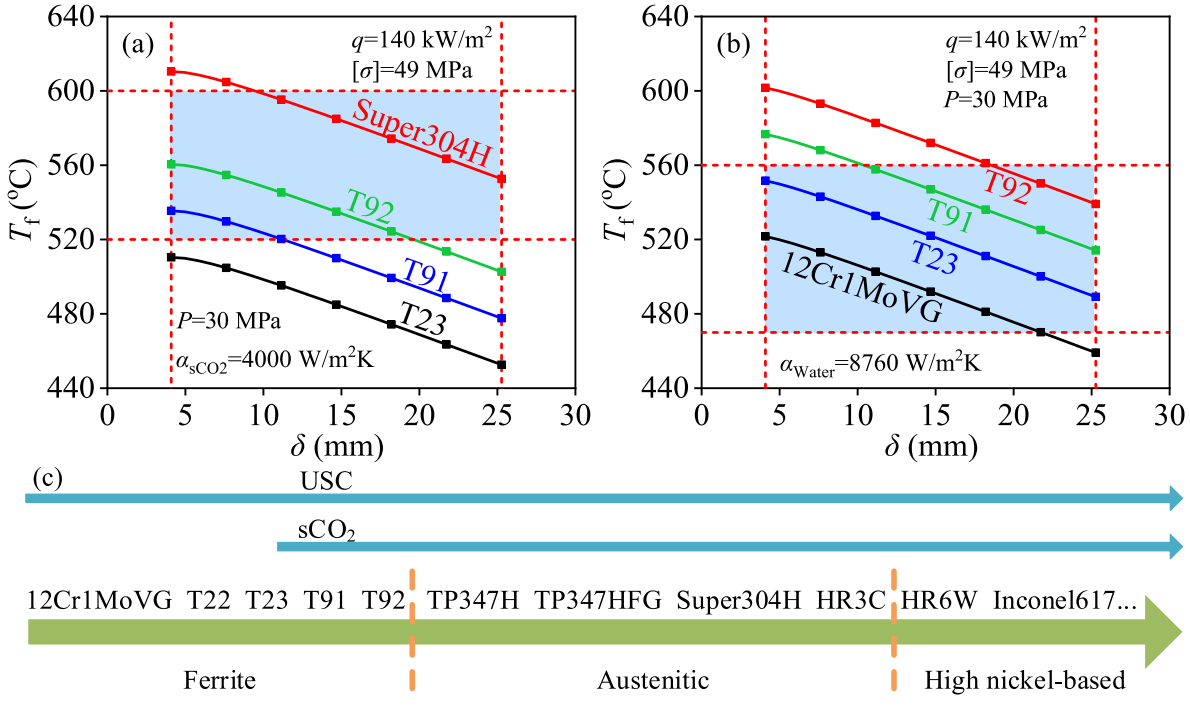

Fig. 5. Selection of sCO_2 and USC boiler heating surface steel.

steel grade for the heating surface of the sCO_2 boiler needs to be raised.

Fig. 6 is a diagram of the heating surface layout of the TCO boiler in the partial flow mode and the conventional single-reheating USC boiler in the total flow mode. For TCO boiler, the cooling wall is coupled with the partial flow and heat load matching, to solve the problem of large mass flow in boiler and high temperature of working fluid in the cooling wall. And the burner zone in the furnace has the highest thermal load, three partial flow is adopted for the primary reheating cooling wall to control the wall temperature and make reheater pressure drop acceptable. For conventional USC boilers, the working fluid inlet temperature of the economizer is among 300–330 °C, and the working fluid temperature in the water wall is generally under 480 °C [37] which is lower than CO_2 entrance temperature of sCO_2 boiler cooling wall.

Table 5 shows the tube specifications, material selection and weight of each heating surface of the TCO boiler and reference USC boiler. It can be seen that the heating surface RH1 and Heater4 at the sCO_2 boiler tail flue have larger weight. In addition, there is a new feature for sCO_2 cycle, the boiler pressure drop will significantly affect the sCO_2 power cycle efficiency, while the water-steam Rankine cycle efficiency is less sensitive to the boiler pressure drop. For the sCO_2 cycle with reheating, the boiler pressure drop can be divided into two parts: the main heater pressure drop and the reheater pressure drop. The former increases the power consumption of the compressor, the later reduces the turbine work. Both can significantly reduce cycle thermal efficiency. When the main heater pressure drop and reheating pressure drop increase by 1 MPa, the cycle thermal efficiency will decrease by 1% and 2%, respectively [19,38]. The reheating pressure drop has a more obvious impact on the cycle efficiency, thus the heating surface of reheating will adopt larger tube diameter (see Table 5).

4.2. The equipment cost estimation and analysis for TCO and USC

Fig. 7a shows the equipment cost share percentage of the TCO and USC. Global system equipment is roughly divided into six categories, namely: boiler, turbine, compressor, recuperator, cooler (USC corresponds to boiler, turbine, pump, heater, condenser) and auxiliary equipment. Fig. 7a indicates that for the TCO, recuperators, boiler and compressors account for the largest proportion, reaches 81.21% of the total equipment cost. In the USC, boiler, turbines and auxiliary equipment account for 89.7% of the total equipment cost. Fig. 7b illustrates the comparison of equipment costs. Compared with the USC, the costs of the boiler, recuperators, compressors and coolers of the TCO have increased significantly. Specifically, the cost of sCO_2 turbine decreases by 30.0%, but recuperator cost of TCO seems to be one magnitude larger than that of USC heater, the cost of sCO_2 boiler increase by 36.3%, the recuperator cost drives up the total cost of TCO. Hence, the total equipment cost of the TCO is extremely higher than the USC, which is 1.92 times of USC.

For the currently developed water-steam Rankine cycle, the heat recovery cost is very low. Thus, the extremely high cost of recuperators induces us to carefully analyze what are the factors that affect the recuperators cost. At high efficiencies, a significant amount of recuperation and small temperature difference of recuperators in sCO_2 power cycle, the cost of recuperators will constitute the major part of the total equipment cost. In TCO, the recuperators cost accounts for 44.02% of the total equipment cost. Here, two aspects affect the recuperator cost which are the performance and the manufacturing level are discussed.

In terms of performance, from the recuperator cost formula, its cost is inversely proportional to its integral average temperature difference. When the heat recovery is constant, the smaller temperature difference, the higher recuperator cost. Fig. 8a shows the change of the integral temperature difference of the recuperator ΔT_{int} with the pinch

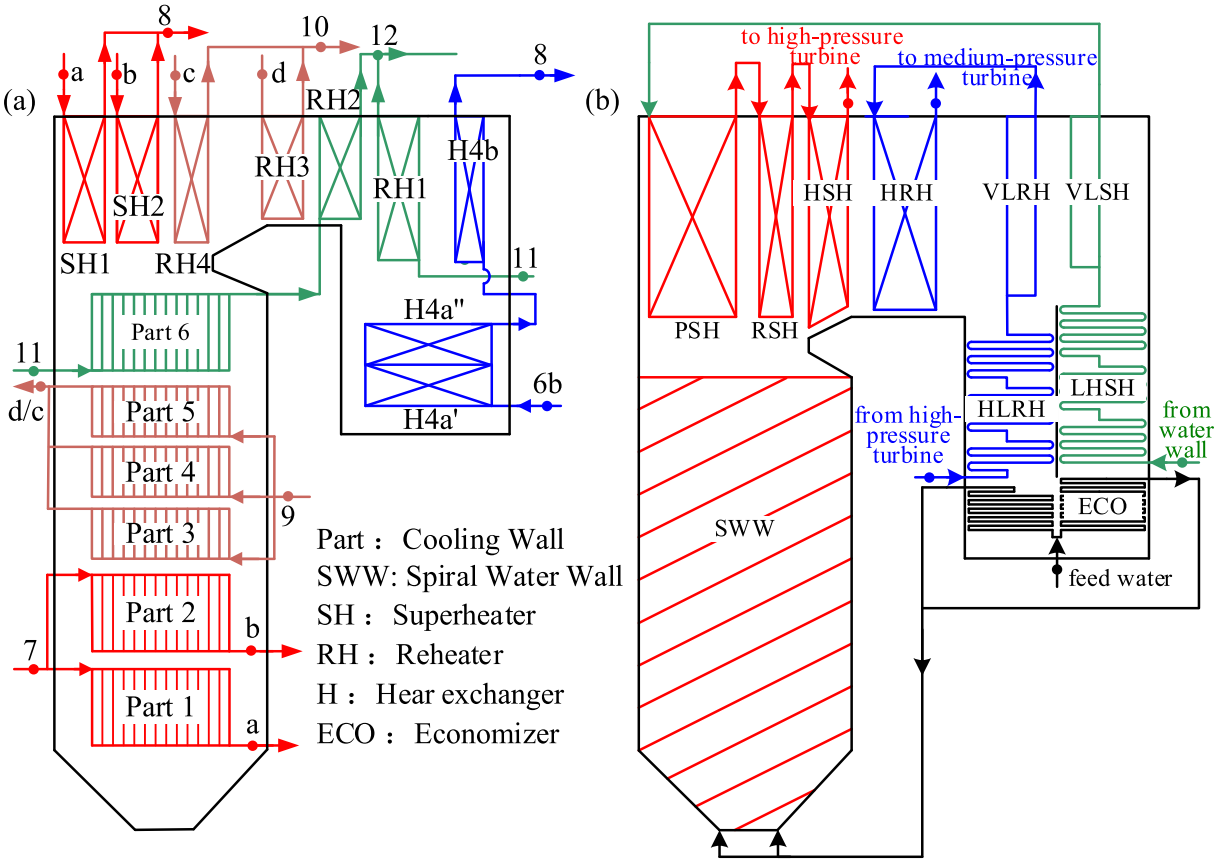

Fig. 6. Heating surfaces layout of TCO boiler and reference single-reheating USC boiler.

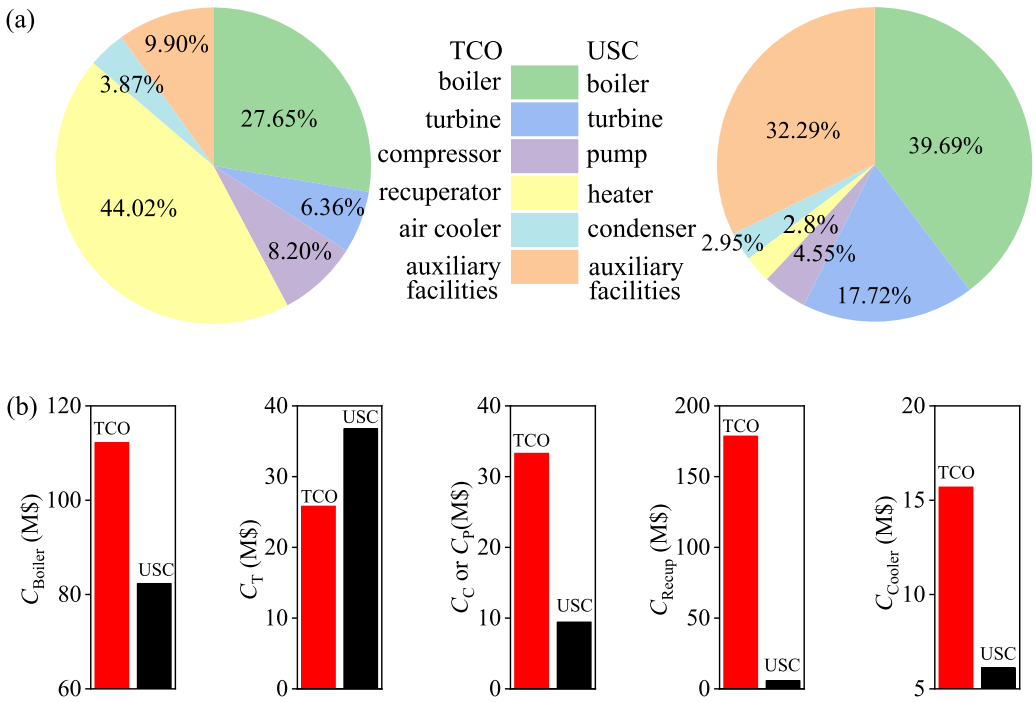

Fig. 7. The equipment cost estimation of TCO and USC (a: main equipment cost ratio; b: comparison of main equipment costs).

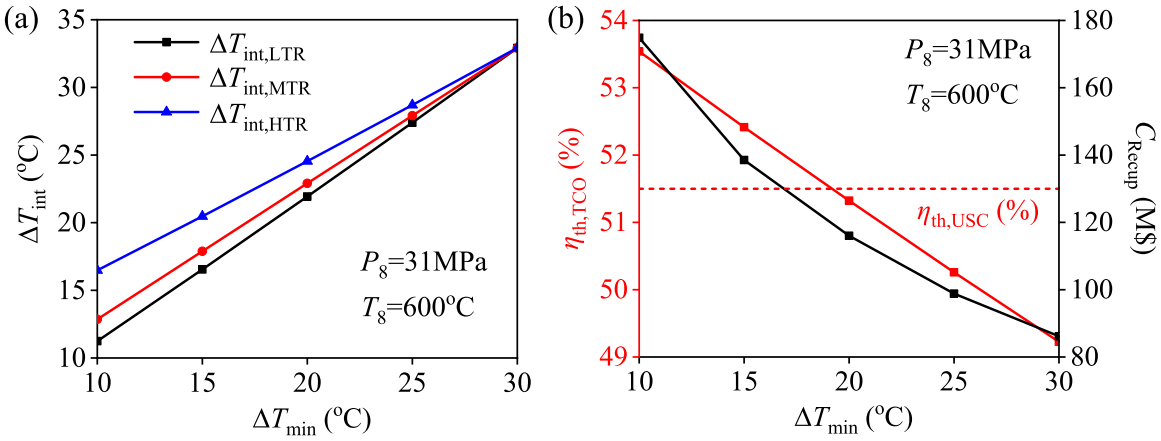

Fig. 8. Pinch temperature impact on integral temperature difference, thermal efficiency and recuperator cost of TCO.

temperature ΔT_{min}. In the low, medium and high temperature recuperator, under the same pinch temperature, the integral temperature difference of the LTR is the smallest, HTR is the largest. With the pinch temperature increases, the integral temperature difference of the three types of recuperators tends to be identical. Furthermore, as shown in Fig. 8b, the pinch temperature not only affects recuperator cost, but also affects cycle efficiency. With the increase of pinch temperature, both the thermal efficiency and recuperators cost of power plant will decrease. However, the decrease of cycle thermal efficiency will increase the coal consumption of the power plant, which will lead to an increase in operation cost. Obviously, the cost advantage and efficiency disadvantage caused by increasing the pinch temperature are mutually restricted, there is the best pinch temperature that makes the system economy optimal.

As far as manufacturing level, the manufacturing technology of recuperators is immature. Therefore, this study will linearly change the fitting coefficient of the recuperator cost formula in the current economic analysis. It can be seen from Fig. 9 when the cost ratio coefficient of recuperators f_{Recup} is decreased from 1 to 0.2, the recuperators cost is reduced from 44.02% to 13.94% of the total equipment cost. Under such condition, the total equipment cost of the TCO may reach the same level as the advanced USC. Analysis shows, high-performance and low-cost recuperators is the keys to large-scale use of sCO_2 power generation systems.

In order to manage the cost of recuperator, the following methods may be adopted in the future.

1) The printed circuit heat exchanger (PCHE) is replaced with other type heat exchanger to save costs of heat recovery. For example, use the periodic flow regenerator instead of the PCHE will result in the

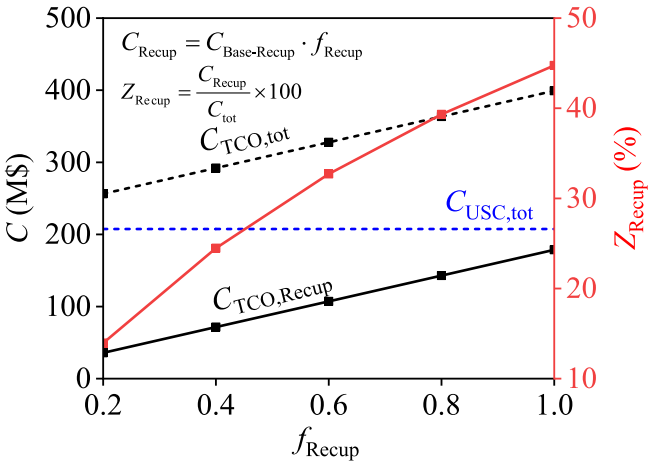

Fig. 9. The regenerator cost varies with the manufacturing level.

increase in heat transfer efficiency and 50% cost reduction [39]; Sandia National Laboratory's new concept heat exchanger CMHE (cast metal heat exchanger), which may provide similar or better performance to PCHE, and the cost is less than 1/5 of PCHE [40].

2) Compared with the HTR, the integral temperature difference of the LTR is small (see Fig. 8a), the pinch temperature of the LTR may be appropriately increased to reduce the heat exchange area and cost.
3) The cost of recuperator also depends on the cycle layout being used, even with the same power output. Different sCO_2 power cycle layouts will have different characteristics of the recuperative system, and the modification of the cycle structure may reduce the cost of the recuperative system [41].
4) Split the HTR into two parts or even more, so that the temperature of the recuperator's steel and CO_2 working fluid can be matched to reduce the cost of the recuperator system. In short, the temperature correction factor f_T in the formula for calculating the recuperator cost is reduced.

4.3. Discussion on calculation results of economic indicators

For two power generation systems, the unit capacity and the vapor parameters are same. It can be seen from Table 6 that the 1000 MW sCO_2 coal-fired power generation system based on triple-compression cycle with overlap energy utilization which power generation efficiency is 49.01%, the 1000 MW ultra-supercritical water-steam coal-fired power generation system is based on 10-stage extraction steam to recover heat which power generation efficiency is 48.12%. As the TCO shows higher efficiency, its coal consumption for power supply b_g is much lower than USC, reflecting the advantage of sCO_2 coal-fired power generation systems. However, the total equipment cost of the TCO is higher than the USC, leading to a higher specific cost (*SC*), which is 1.29 times of the USC, damaging the superiority of sCO_2 coal-fired power generation systems. In order to make the sCO_2 power generation systems economically feasible and competitive, the capital cost of equipment needs to be reduced from present estimates.

Table 6
Performance comparison of TCO and Huaneng Laiwu USC [20].

	sCO_2	USC
Net power W_{net}(MW)	1000	1000
House power L_{fcy} (%)	1.48	3.97
Cycle thermal efficiency η_{th} (%)	53.54	52.45
Boiler efficiency η_b(%)	94.43	94.65
Power generation efficiency η_{cp} (%)	49.01	48.12
Specific cost *SC*($/kW)	693.87	531.50
Coal consumption for power supply b_g(g/kWh)	245.26	266.75
Levelized cost of electricity *LCOE*($/MWh)	60.56	61.37

Note: $\eta_{cp} = \eta_{th}\eta_m\eta_g\eta_p\eta_b$, η_{th}, η_m, η_g, η_p, η_b, respectively, thermal efficiency, mechanical efficiency, generator efficiency, pipeline efficiency and boiler efficiency.

For the purpose of comprehensively weight equipment investment cost and operation cost of system, here, the levelized cost of electricity (*LCOE*) is selected as a measurement to evaluate the profitability of power plants. As shown in Fig. 10, the *LCOE* of the TCO is 1.32% lower than the advanced USC. It can be seen that fuel cost account for the highest proportion in two systems, reaching 60–70% of the total cost, and O&M costs account for the smallest. Compared with USC, the decrease in *LCOE* of TCO is mainly due to fuel cost reduction by efficiency increment which is up to 8%, and the system efficiency advantage is sufficient to make up for the drawback caused by the increase of the annual investment cost.

4.4. Sensitivity analysis of key economic factors

A sensitivity analysis conducted on various key economic factors, and the economics of TCO assessed from different perspectives. Fig. 7a presented that the recuperators cost accounts for the largest proportion of the TCO total equipment cost. The recuperators cost in the current economic analysis contains uncertainties, thus its sensitivity analysis is necessary. Fig. 11 is further explained the influence of the recuperators cost on the *FCI* and *LCOE* estimation results. With the advancement of compact heat exchangers, the cost ratio coefficient of recuperators f_{Recup} will decrease, and the *FCI* of TCO is sharply reduced. The *LCOE* of TCO gradually decreases due to lessen of *FCI*. When the f_{Recup} is decreased from 1 to 0.2, the *LCOE* of the TCO is reduced from 60.56 to 57.05 $/MWh. Compared with the *LCOE* of the USC (61.37$/MWh), when f_{Recup} is 0.2, the *LCOE* of the TCO is reduced by 7.05%. Apparently, reducing the cost of recuperator is the key to secure the economic superiority of sCO_2 coal-fired power generation systems.

We note that fuel costs almost 60–70% of the *LCOE*, and changes in coal prices will induce a magnitude effect on *LCOE*. Exploring the impact of coal price changes on *LCOE* is important for the development of sCO_2 coal-fired power generation systems. Fig. 12a shows the variation of *LCOE* of the TCO and USC with coal price fluctuation. Due to the lower power generation efficiency of USC, it is more sensitive to coal price changes. With the gradual increase of the coal price ratio coefficient f_{coal}, coal price rises, the *LCOE* difference between TCO and USC rises, which enhances the economic benefit of sCO_2 coal-fired power generation systems.

The annual utilization factor of power plant *w* is directly related to the annual power generation, which affects the profitability of the power plants. Fig. 12b shows sensitivity analysis from an operational standpoint, when *w* is about 0.67, the *LCOE* of the TCO is almost the same as USC. As *w* continues to decrease, the *LCOE* of the TCO is higher than that of USC even if the TCO efficiency is higher. This is because the annual power generation and annual fuel consumption are cut back, and the fuel cost reduction brought by the high efficiency has no ascendancy

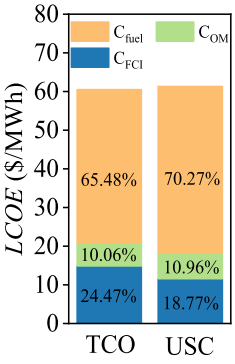

Fig. 10. *LCOE* (levelized cost of electricity) estimation results of TCO and USC.

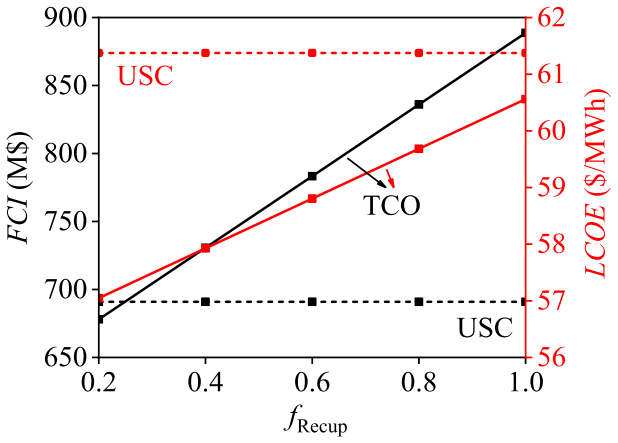

Fig. 11. Effect of recuperator manufacturing level on *LCOE*.

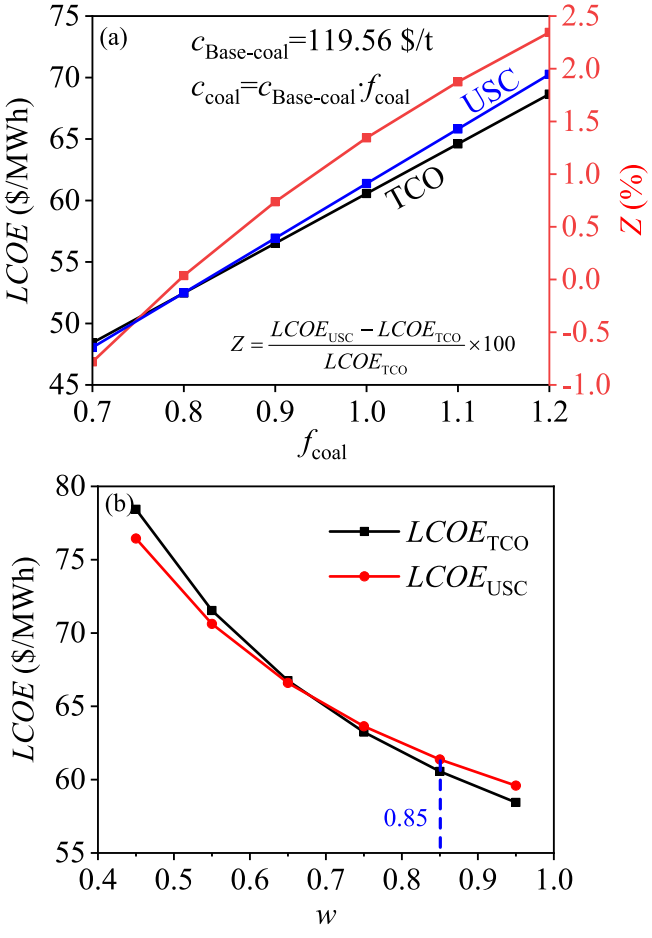

Fig. 12. Key economic factors versus *LCOE* (a: coal price; b: annual utilization factor).

compared with the lager annual investment cost. Corresponding, in order to ensure that sCO_2 coal-fired power generation systems are economically viable, *w* must be maintained above 0.67. The *w* reference in this study is 0.85. Under the same assumptions, the TCO performs better in terms of thermodynamic performance and economy.

5. Conclusion

We investigated the economics of sCO_2 and ultra-supercritical water-steam coal-fired power generation system, respectively. The following conclusions are drawn.

The sCO_2 boiler cost has increased by 36.3% compared with the water-steam boiler cost. The increase in heating surface steel grade and thick, lower CO_2 heat transfer capacity, and complex boiler structure are the reasons for the cost increasing. Partial flow and heat load matching of the heating surface are proposed to reduce its cost.

The recuperator cost is the largest in sCO_2 cycle total equipment cost. The sCO_2 system economy is constrained by the recuperator pinch temperature, a most economical system is obtained at an optimal pinch temperature.

In this study, the power generation efficiency of TCO and USC are 49.01% and 48.12%, respectively. The TCO has higher *SC*, which is 1.29 times than the reference USC, and the *LCOE* is 60.56 $/MWh, with a 1.32% lower compared to USC. The TCO performs better in terms of thermodynamic performance and economy.

Sensitivity analysis on recuperator cost, coal price and the annual utilization coefficient of power plant points out the development direction for improving the sCO_2 coal-fired power generation system economic competitiveness.

CRediT authorship contribution statement

Jinliang Xu: Conceptualization, Methodology, Supervision, Software. **Xue Wang:** Data curation, Writing - original draft. **Enhui Sun:** Visualization, Investigation, Software, Validation. **Mingjia Li:** Writing - review & editing.

Declaration of Competing Interest

The authors declare that they have no known competing financial interests or personal relationships that could have appeared to influence the work reported in this paper.

Acknowledgements

The study was supported by the National Key R&D Program of China (2017YFB0601801), and the Natural Science Foundation of China (51821004).

References

[1] BP Statistical Review of World Energy, 2020.
[2] Verdolini E, Vona F, Popp D. Bridging the gap: Do fast-reacting fossil technologies facilitate renewable energy diffusion? Energ Policy 2018;116:242–56.
[3] Dostal V, Hejzlar P, Driscoll MJ. The supercritical carbon dioxide power cycle: Comparison to other advanced power cycles. Nucl Technol 2006;154:283–301.
[4] Xu J, Liu C, Sun E, Xie J, Li M, Yang Y, et al. Perspective of S−CO_2 power cycles. Energy 2019;186:115831.
[5] Holcomb GR, Carney C, Doğan ÖN. Oxidation of alloys for energy applications in supercritical CO_2 and H_2O. Corros Sci 2016;109:22–35.
[6] Feher EG. The supercritical thermodynamic power cycle. Energy Convers Manage 1968;8:85–90.
[7] Iverson BD, Conboy TM, Pasch JJ, Kruizenga AM. Supercritical CO_2 Brayton cycles for solar-thermal energy. Appl Energy 2013;111:957–70.
[8] Moisseytsev A, Sienicki JJ. Investigation of alternative layouts for the supercritical carbon dioxide Brayton cycle for a sodium-cooled fast reactor. Nucl Eng Des 2009;239:1362–71.
[9] Park JH, Park HS, Kwon JG, Kim TH, Kim MH. Optimization and thermodynamic analysis of supercritical CO_2 Brayton recompression cycle for various small modular reactors. Energy 2018;160:520–35.
[10] Le Moullec Y. Conceptual study of a high efficiency coal-fired power plant with CO_2 capture using a supercritical CO_2 Brayton cycle. Energy 2013;49:32–46.
[11] Mecheri M, "SCO2 closed Brayton cycle for coal-fired power plant," in 2nd European sCO2 Conference 2018. Essen, Germany, (2018).
[12] Park S, Kim J, Yoon M, Rhim D, Yeom C. Thermodynamic and economic investigation of coal-fired power plant combined with various supercritical CO_2 Brayton power cycle. Appl Therm Eng 2018;130:611–23.
[13] Li M, Wang G, Xu J, Ni J, Sun E. Life cycle assessment analysis and comparison of 1000 MW S-CO_2 coal fired power plant and 1000 MW USC water-steam coal-fired power plant. J Therm Sci 2020.
[14] Zhu M, Zhou J, Su S, Xu J, Li A, Chen L, et al. Study on supercritical CO_2 coal-fired boiler based on improved genetic algorithm. Energ Convers Manage 2020;221:113163.

[15] Weiland NT, Lance BW, Pidaparti SR. sCO2 Power Cycle Component Cost Correlations From DOE Data Spanning Multiple Scales and Applications. Proceedings of the Asme Turbo Expo: Turbomachinery Technical Conference and Exposition, 2019, Vol 9. (2019).
[16] Sun E, Xu J, Hu H, Li M, Miao Z, Yang Y, et al. Overlap energy utilization reaches maximum efficiency for S-CO_2 coal fired power plant: A new principle. Energ Convers Manage 2019;195:99–113.
[17] Sun E, Xu J, Li M, Li H, Liu C, Xie J. Synergetics: The cooperative phenomenon in multi-compressions S-CO_2 power cycles. Energy Convers Manage: X 2020;7:100042.
[18] Ahn Y, Bae SJ, Kim M, Cho SK, Baik S, Lee JI, et al. Review of supercritical CO_2 power cycle technology and current status of research and development. Nucl Eng Technol 2015;47:647–61.
[19] Xu J, Sun E, Li M, Liu H, Zhu B. Key issues and solution strategies for supercritical carbon dioxide coal fired power plant. Energy 2018;157:227–46.
[20] Fan H, Zhang Z, Dong J, Xu W. China's R&D of advanced ultra-supercritical coal-fired power generation for addressing climate change. Therm Sci Eng Prog 2018;5:364–71.
[21] Tumanovskii AG, Shvarts AL, Somova EV, et al. Review of the coal-fired, over-supercritical and ultra-supercritical steam power plants. Therm Eng 2017;64:83–96.
[22] Liu C, Xu J, Li M, Wang Z, Xu Z, Xie J. Scale law of sCO_2 coal fired power plants regarding system performance dependent on power capacities. Energ Convers Manage 2020;226:113505.
[23] Guide on selection of furnace characteristic parameters for large pulverized coal fired boilers. Power industry standards of P.R.C, DL/T 831-2015 [in Chinese].
[24] Liu Z, He Y, Qu Z, et al. Experimental study of heat transfer and pressure drop of supercritical CO_2 cooled in metal foam tubes. Int J Heat Mass Tran 2015;85:679–93.
[25] Dittus FW, Boelter LMK. Heat transfer in automobile radiators of the tubular type. Int Commun Heat Mass 1985;12:3–22.
[26] Jiang P, Zhang L, Xu R. Experimental study of convective heat transfer of carbon dioxide at supercritical pressures in a horizontal rock fracture and its application to enhanced geothermal systems. Appl Therm Eng 2017;117:39–49.
[27] Fan Q. Design and operation of ultra-supercritical boiler. China Electric Power Press 2010 [in Chinese].
[28] Subbaraman G, Kung S, Saari H. Materials for supercritical CO_2 applications. 6th International sCO_2 Power Cycles Symposium. 2018.
[29] Zima W, Nowak-Ocłoń M, Ocłoń P. Novel online simulation-ready models of conjugate heat transfer in combustion chamber waterwall tubes of supercritical power boilers. Energy 2018;148:809–23.
[30] Zhao Q, Gu H, Lu Y. Some developments of heat-resistant steel for power plant boilers abroad. J Power Eng 1998;01:74–83.
[31] Viswanathan R, Sarver J, Tanzosh JM. Boiler materials for ultra-supercritical coal power plants—Steamside oxidation. J Mater Eng Perform 2006;15:255–74.
[32] EPPEI. Reference cost index of thermal power project quota design (Level 2017). China Electric Power Plann Eng Inst 2018.
[33] Marchionni M, Bianchi G, Tassou SA. Techno-economic assessment of Joule-Brayton cycle architectures for heat to power conversion from high-grade heat sources using CO_2 in the supercritical state. Energy 2018;148:1140–52.
[34] Calculating method of economical and technical index for thermal power plant. National Energy Administration; 2015.
[35] Xu G, Xu C, Yang Y, Fang Y, Zhou L, Zhang K. Novel partial-subsidence tower-type boiler design in an ultra-supercritical power plant. Appl Energ 2014;134:363–73.
[36] James R, Zoelle A, Keairns D. Cost and performance baseline for fossil energy plants volume 1: bituminous coal and natural gas to electricity. NETL 2019.
[37] Zhao Q, Zhu L. Research on heat resistant steels for supercritical boiler. Machine Indust Press 2010 [in Chinese].
[38] Li H, Zhang Y, Yang Y, Han W, Yao M, Bai W, et al. Preliminary design assessment of supercritical CO_2 cycle for commercial scale coal-fired power plants. Appl Therm Eng 2019;158:113785.
[39] Hinze JF, Nellis GF, Anderson MH. Cost comparison of printed circuit heat exchanger to low cost periodic flow regenerator for use as recuperator in a s-CO2 Brayton cycle. Appl Energ 2017;208:1150–61.
[40] Carlson MD, Kruizenga AK, Schalansky C, Fleming DF. Sandia progress on advanced heat exchangers for SCO2 Brayton cycles. 4th International sCO_2 Power Cycles Symposium. 2014.
[41] Zada KR, Kim R, Wildberger A, Schalansky CP. Analysis of supercritical CO_2 Brayton cycle recuperative heat exchanger size and capital cost with variation of layout design. 6th International sCO_2 Power Cycles Symposium. 2018.